

IN VIVO QUANTIFICATION OF RENAL SODIUM CONCENTRATION WITH A DUAL RF RESONATOR SYSTEM

R. Kalayciyan¹, F. Wetterling¹, S. Neudecker², and L. R. Schad¹

¹Computer Assisted Clinical Medicine, Heidelberg University, Mannheim, Germany, ²Medical Research Center, Heidelberg University, Mannheim, Germany

Introduction:

The quantification of local Tissue Sodium Concentration (TSC) levels can serve as a diagnostic measure for renal diseases, because TSC is strongly linked to the corticomedullary function, which regulates the vascular ion concentrations [1, 2]. However, the validation of the achieved TSC quantification accuracy on rat kidneys using quantitative ²³Na Magnetic Resonance Imaging (qNa-MRI) technique is challenging and results in low SNR in acquired ²³Na images. Additionally, homogeneous B₁-field is required for quantification of the TSC. Although surface coils provide high SNR, the generated B₁-field of a surface coil is highly inhomogeneous. Therefore, the aim of this work was to develop a dual RF resonator system composed of a noise-matched receive-only surface coil and a commercial double-tuned ¹H/²³Na transmit volume resonator in order to maximize signal sensitivity as well as the B₁-field homogeneity for TSC measurements in *in vivo* rat kidneys.

Methods:

Noise-matching via low noise preamplifiers (LNPs) introduced by Roemer *et al.* is a commonly used concept for decoupling multiple receiver elements in phased array coils [3]. In this work, the developed ²³Na receive-only surface coil was designed to be a single-coil element (rectangular 25mm x 50mm). The LNP (MwT, USA, 2.1 Ω input impedance, 29 dB gain, 0.5 noise figure) was noise-matched to the detector element via a $\lambda/4$ transformation network, while the by Reykowski *et al.* [4] suggested pi-transformation-network was modified with the intention to minimize the number of electronic circuit components. Thus, the loop-coil was noise-matched to the required 50 Ω input impedance of the preamplifier, which when connected to the transformation network presents high impedance to the coil at its terminals. During the design the transformation path of the network was adjusted to the resonance frequency of 105 MHz. The efficiency of this trap circuit was measured by a S₂₁ measurement with decoupled probe pair (4 cm \varnothing) brought to near proximity of the receive-only coil: The peak split was measured to be 20 MHz and -45 dB preamplifier decoupling was achieved. Furthermore, passive decoupling circuit was added to the coil circuit to compensate for imperfect geometric decoupling of the surface coil from the volume resonator. The birdcage resonator's B₁-field was orthogonally arranged to the surface coil's B₁-field in order to maximize the geometric decoupling. The ²³Na-imaging performance of the LNP coil was compared to a home-built transceiver surface coil (Q_{loaded} / unloaded = 100 / 112) with the identical detector dimensions. A cylindrical tube of 4 cm \varnothing filled with 155 mMol/l NaCl solution was scanned with 3D-GRE sequence on a 9.4 T system (Bruker BioSpin GmbH, Ettlingen, Germany) with TE/TR = 3ms/20ms, voxel size = 1 x 1 x 2.6 mm, and an acquisition time of 10 min (Fig. 1a-c). To provide a comparable situation for both coil system sensitivities, the phantom experiments were performed in existence of the volume resonator for both transceiver (TxRx) and transmit-only-receive-only (ToRo) measurements. A further measurement was performed using the double-tuned ²³Na/¹H transceiver volume resonator (Bruker BioSpin GmbH, Ettlingen, Germany) with inner diameter 72mm in order to estimate its B₁-field homogeneity (see Fig. 1c). The flip angle calibration for the ToRo and volume transceiver coil experiments was straight forward, but for the transceiver surface coil inhomogeneous B₁-field hampered exact flip angle calibration so that the 90° flip angle had to be set in approximately 4mm distance from the surface coil's detector element. The SNR values were plotted as a function of depth along the vertical profile through the centre of the object and are graphed in Fig. 1d. In order to quantify the TSC the surface coil's receive sensitivity was compensated for through a reference scan method [5]. A homogeneous reference phantom was scanned in addition to the two fiducial vials (155 mMol NaCl), which were permanently fixed on top of the receiver coil (see Fig. 2b, d). Sample and reference scans were co-registered to the reference vial positions before the sensitivity corrected ²³Na image was computed as the quotient image (Fig. 2c) from the sample and the reference scans, respectively. Differences in coil loading between both sample and reference scan were compensated for by a correction factor [6]. To demonstrate the proof-of-concept, TSC quantification accuracy was verified for imaging of a concentration phantom containing gels of various NaCl and agarose concentrations (40-160 mM NaCl in 0-5% agarose gel) shown in Fig. 2a. ¹H-reference scan was recorded with ²³Na/¹H transceiver volume resonator by means of a 3D-Flash sequence using TE/TR = 3 / 20 ms, anisotropic resolution of 0.5x0.5x1mm³, and Tacq = 3 min. 3D-UTE sequence which is an FID readout technique - sampling the *k*-space in a radial manner starting from the *k*-space center [7] - was used for *in vivo* and phantom ²³Na MRI acquisitions. The radial 3D ultra-short TE (3D-UTE) sequence is less prone to motion artifacts than the 3D-Gradient Echo (GRE) sequence, and the fact that 3D-UTE allowed for short TE < 0.1 ms. A healthy female rat (~350 g) was imaged *in vivo* with following sequence parameters: isotropic 1mm³ voxel size, TR = 60 ms, Tacq = 13 min, BW = 5 kHz, 0.1 ms block pulse length, FOV = 6.4 cm³ and TE_{UTE} = 60 μ s.

Results and Discussion:

The dual RF resonator system for ²³Na MRI comprised a modified concept for noise-matching the ²³Na receive-only surface coil to the LNP. In conjunction with the volume resonator, optimum B₁-field homogeneity was generated, while high SNR ²³Na images could be acquired - an essential aspect for the quantification of TSC in the rat kidney. The SNR of the TxRx surface coil was measured to be approx. 15% lower compared to the ToRo system which may be the result of undesired coupling with the volume resonator that was left inside the magnet during the TxRx measurement (see Fig. 1d). Furthermore, the ToRo system achieved slightly better penetration into depth of the sample which is a consequence of the provided homogeneous B₁-field by the volume resonator in this mode. The quantitative measurements of known phantom ²³Na concentrations resulted in reasonably good quantification precision of ± 10 %. After verification of the quantification technique on a phantom, *in vivo* TSC was quantified for a healthy rat (see Fig. 3 - right). The corticomedullary TSC gradient with 90 mM TSC maximum is well-recognizable in the TSC map of the rat kidney (Fig. 3c). Using short TE (60 μ s) in combination with relatively long TR (60 ms) enabled the TSC quantification without the need to compensate for T1 or T2 relaxation effects. However, the quantification method, especially the co-registration of the reference and sample images, is prone to errors caused by the close positioning of the fiducial vials to the resonator and consequently the variation in the B₁-field in these regions. Future quantification studies need to include a third vial with known ²³Na concentration within the field of view to improve the TSC quantification accuracy.

References:

[1] Maril *et al.*, Kidney Int. 69:765-768 (2006); [2] Maril *et al.*, Kidney Int. 65:927-935 (2004); [3] Roemer *et al.*, MRM, 16(2):192-225 (1990); [4] Reykowski *et al.*, MRM, 33(6):848-852 (1995); [5] Wetterling *et al.*, Proc. ISMRM 18 (2010); [6] Ouwerkerk *et al.*, Breast Cancer Res Treat. 106 (2007); [7] Rahmer *et al.*, MRM 55:1075-1082 (2006).

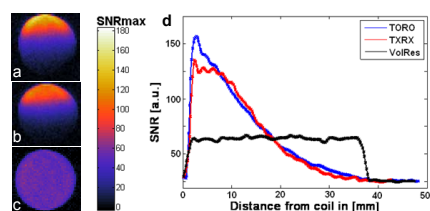


Fig. 1: SNR maps for a) dual resonator (ToRo) system, b) transceiver surface coil (TxRx) with identical detector element dimensions, c) commercial TxRx birdcage volume resonator (VolRes) using 3D-GRE, and d) SNR as a function of depth for ToRo, TxRx surface, and TxRx birdcage (VolRes).

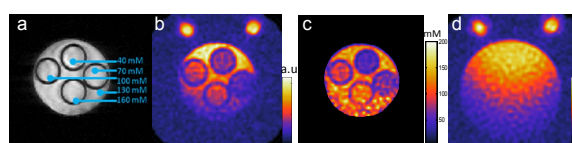


Fig. 2: a) ¹H 3D-GRE image, b) ²³Na 3D-UTE MR images, and c) masked ²³Na concentration map of the resolution phantom. (d) ²³Na image of the homogeneous reference phantom.

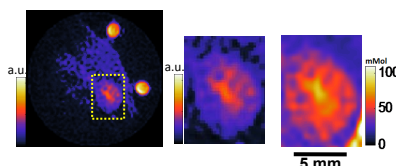


Fig. 3: ²³Na image of an axial cross section through the left kidney image (left). The same image but zoomed into the region of the kidney (centre), and TSC map of *in vivo* kidney (right).